Short Communication

Electrochemical behaviour of spinel LiMn$_2$O$_4$ as positive electrode in rechargeable lithium cells

Li Feng, Yuqin Chang, Lie Wu, Tianhong Lu

Changchun Institute of Applied Chemistry, Changchun 130 022, People's Republic of China

Abstract

The spinel, lithium intercalation compound LiMn$_2$O$_4$ is prepared and studied using the techniques of a.c. impedance and cyclic voltammetry. The impedance behaviour of the LiMn$_2$O$_4$ electrode varies as lithium ions are intercalated or de-intercalated. The reversible behaviour of lithium ions in the LiMn$_2$O$_4$ electrode is confirmed by the results of cyclic voltammetry.

Keywords: Spinel lithium–manganese oxides; Lithium cells; Cyclic voltammetry; A.c. impedance; Fractal theory

1. Introduction

Spinel structure Li–Mn–O compounds are most promising as lithium insertion electrode materials for rechargeable lithium batteries. They are being developed because of the following advantages: (i) a lower overall electrode cost compared with LiNiO$_2$ or LiCoO$_2$; (ii) a high cell voltage; (iii) a long cycle life, and (iv) non-toxicity. Goodenough and co-workers [1,2] observed the reversible intercalation of lithium ions in the spinel structure LiMn$_2$O$_4$ and showed the existence of two reversible intercalation plateaus at 4.1 and 3.0 V versus Li/Li$^+$. Tarascon and co-workers [3–5] conducted many investigations on the preparation of the spinel LiMn$_2$O$_4$, as well as on the charge/discharge behaviour of cells that employed this material. Despite a considerable number of studies on the electrochemical behaviour of LiMn$_2$O$_4$, the compound is still receiving much attention in efforts to improve its cycle life. On the other hand, there have been fewer studies on the properties of the interface between the LiMn$_2$O$_4$ electrode and the electrolyte during the charge/ discharge processes of an Li/EC–DEC–LiPF$_6$/ LiMn$_2$O$_4$ cell (EC = ethylene carbonate; DEC = diethyl carbonate). Such work is important in order to understand the electrochemical behaviour of the spinel LiMn$_2$O$_4$ material as a positive electrode.

In this paper, the preparation of the spinel LiMn$_2$O$_4$ compound is reported. The electrochemical behaviour of an Li/ organic electrolyte/LiMn$_2$O$_4$ cell is evaluated by cyclic voltammetry and a.c. impedance.

2. Experimental

The compound LiMn$_2$O$_4$ was prepared by reaction of LiOH (or LiNO$_3$) with MnO$_2$ powder (>300 mesh) in air; the ratio of the two materials was 7:3. The rate of temperature rise was maintained at 10 °C/h over the 350–550 °C range. This provided sufficient time for the molten LiNO$_3$ salt to mix with the MnO$_2$ particles. The temperature was increased continuously from 550 to 800 °C (or 700 °C) at 50 °C/h, and then kept constant for about 50 h at 800 or 700 °C. The rate of temperature decrease was also controlled at 10 °C/h until the temperature reached the ambient value. The structure of the product was characterized by powder X-ray diffraction (XRD).

The positive electrode consisted of 80 wt.% LiMn$_2$O$_4$ and 20 wt.% teflonized acetylene black, and was pressed on a nickel metal net with dimensions 4 mm × 5 mm. The electrolyte solution was EC + DEC(1:1) + 1 M LiPF$_6$ (or EC + PC(1:1) + 1 M LiPF$_6$). Lithium metal foils were used as the counter and the reference electrodes during electrochemical measurements. Cyclic voltammetry was carried out with a Model 533 potentiostat at a scanning rate of 0.1 mV s^{-1}. The properties of the interface between the LiMn$_2$O$_4$ electrode and the electrolyte for different amounts of lithium intercalation were analysed by a.c. impedance spectroscopy over a frequency range of 100 kHz to 0.01 Hz. This was achieved with a 5208 Two Phase Lock-in Analyzer that was coupled to a Model 273 potentiostat/galvonostat and controlled by an IBM computer.

3. Results and discussion

3.1. XRD of LiMn₂O₄ sample

According to the method of preparation described above, powder samples of $LiMn_2O_4$ were produced and then characterized by XRD, as shown in Fig. 1. It was easily found that almost all of the diffraction peaks were attributable to the spinel structure of $LiMn_2O_4$. The crystal data of the samples are nearly the same as those of standard $LiMn_2O_4$. The band of peaks for the sample prepared at 700 °C (Fig. 1(a)) is a little wider than that at 800 °C (Fig. 1(b)). This may be related to a difference in the size of the particles of the products prepared at different reaction temperatures.

3.2. Cyclic voltammetric measurements

Figs. 2 and 3 show the cyclic voltammograms (CVs) for $Li/EC–DEC–LiPF_6/LiMn_2O_4$ and $Li/PC–DEC–LiPF_6/LiMn_2O_4$ cells with a potential limitation of 3.5 to 4.35 V versus Li/Li^+. There are two redox couples between 3.9 and 4.2 V. This appears not to be in accordance with a one-electron transfer mechanism in rechargeable lithium batteries.
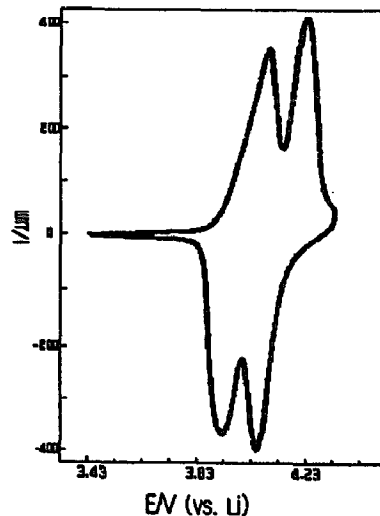

Fig. 2. Cyclic voltammogram for $Li/PC–EC–1$ M $LiPF_6/LiMn_2O_4$ cell; scan rate $= 0.1$ mV s^{-1}.

It is often considered that lithium ions are intercalated from the electrolyte into the tetrahedral $8a$ sites of the $LiMn_2O_4$ spinel structure. When a small number of Li^+ ions are moved
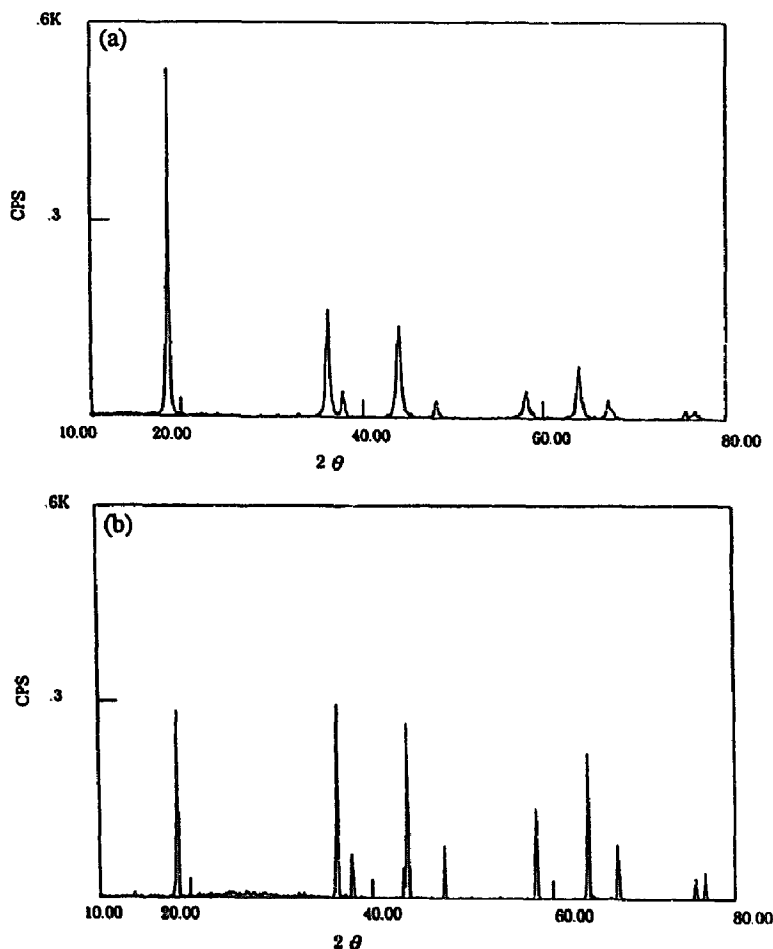

Fig. 1. X-ray powder diffraction pattern for spinel structure $LiMn_2O_4$ prepared at: (a) 700 °C, and (b) 800 °C.
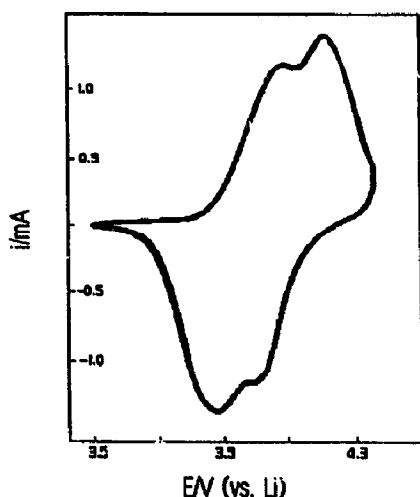
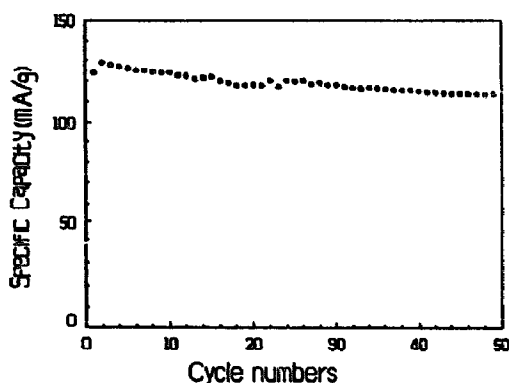Fig. 3. Cyclic voltammogram for Li/DEC–EC–1 M LiPF$_6$/LiMn$_2$O$_4$ cell; scan rate = 0.1 mV s^{-1}.

Fig. 4. Variation of capacity of Li/EC–DEC–LiPF$_6$/LiMn$_2$O$_4$ cell as a function of cycle number; discharge rate = 0.2 mA cm^{-2}.

into the tetrahedral sites of the spinel structure, the repulsion between adjacent lithium ions is weak. With increase of Li$^+$ ions into the tetrahedral sites, the activity of each Li$^+$ ion will be influenced by the four Li$^+$ ions that surround it. As a result of this interaction between the lithium ions, the peak splits into two on the CV curves. The energy for the split of the peak can be calculated; it is about 0.02 eV for each Li–Li. By contrast, when the LiMn$_2$O$_4$ electrode is oxidized, two related oxidation peaks appear on the CV curves. This indicates that the Li$^+$ ions move out from the sites of the spinel structure. The peak split is also accompanied by the appearance of two stages at about 4.1 V on the typical charge/discharge curve of the Li/LiMn$_2$O$_4$ cell. For both the electrolyte systems, viz., EC–DEC–LiPF$_6$ and PC–DEC–LiPF$_6$, the spinel structure of LiMn$_2$O$_4$ displays reversible lithium intercalation/de-intercalation, as shown in Figs. 2 and 3.

The variation in capacity as a function of charge/discharge number for an Li/EC–DEC–LiPF$_6$/LiMn$_2$O$_4$ cell is shown in Fig. 4. The discharge capacity reaches a maximum value (129 mAh g^{-1}) on the second or third cycle, and then decreases slowly with cycling at a rate of 0.2 mA cm^{-2}. After

cycle 50, the capacity has decreased to 113 mAh g^{-1}, i.e., 13% lower than the maximum value.

3.3. A.c. impedance measurements

The a.c. impedance technique provides information on the charge transfer and diffusion of lithium ions in both the surface layer and the interior of the LiMn$_2$O$_4$ electrodes. A.c. impedance studies were conducted on an Li/EC–DEC–LiPF$_6$/LiMn$_2$O$_4$ cell under different conditions of discharge/charge in order to observe the behaviour of Li$^+$ ion intercalation and de-intercalation. The results are presented in Fig. 5. The impedance spectra (a), (b) and (c) were measured when the cell was discharged to 4.15, 3.54 and 3.16 V, respectively, during the first discharge. The spectrum (d) corresponds to charging of the cell to 4.16 V. In Fig. 5(a), the impedance spectrum consists of two semi-circles and a 'spur' with a slope of about 45°. The electric capacities of the semicircles are 6.0 × 10^{-5} and 2 × 10^{-2} F cm^{-2}. Therefore, it is concluded that the semi-circle in the high-frequency zone results from an interfacial charge-transfer impedance between the electrolyte and the LiMn$_2$O$_4$ electrode. The semi-circle at low frequency is related to Li$^+$ ion diffusion from the surface of the electrode to inside the spinel structure of the LiMn$_2$O$_4$. Both of the impedances are small (< 100 Ω), as indicated by their semi-circle diameters. Although the 'spur' at the right of the spectrum is not apparent, it still shows a diffusion-determining step during discharge of the cell. With further discharge, spectra (b) and (c) reveal that the semi-circle at low frequency disappears and changes to a long 'spur'. This means that diffusion of Li$^+$ ions into the spinel structure becomes more difficult. Furthermore, the 'spur' inclines towards the imaginary axis after discharge of the cell. According to fractal theory and Moive's formula [6]
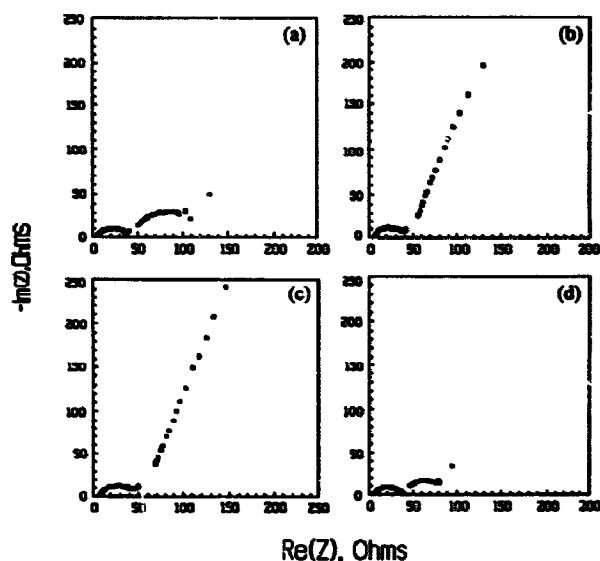

Fig. 5. A.c. impedance spectra of Li/EC–DEC–LiPF$_6$/LiMn$_2$O$_4$ cell at different OCVs: (a) 4.15 V; (b) 3.54 V; (c) 3.16 V, and (d) 4.16 V; frequency range: 10 kHz to 0.01 Hz.
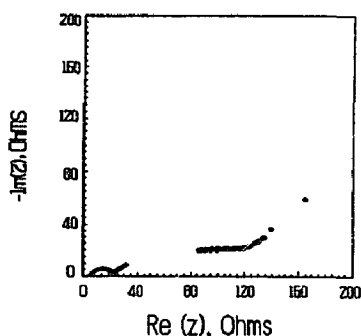
Fig. 6. A.c. impedance spectrum of Li/EC–DEC–LiPF$_6$/LiMn$_2$O$_4$ cell after 46 cycles.

$$n = 1 - 2\alpha/\pi \qquad (1)$$

where n is the fractal exponent, and α is the constant phase angle formed by the spur line and the imaginary axis direction, and is $< 45°$ after discharge. The fractal exponent n has a value between 0.5 and 1 during the discharge process of the cell. This indicates a variation in the surface morphology of the LiMn$_2$O$_4$ electrode, that is, the surface of the electrode is becoming more rough. This behaviour hinders movement of the Li$^+$ ions to the 8a sites of the spinel structure. On the other hand, when the electrode is charged to the original open-circuit voltage (OCV), i.e. $V_{OCV} = 4.16$ V, the impedance spectrum in Fig. 5(d) is similar to that before discharge, as shown in Fig. 5(a). On the other hand, spectrum (d) becomes smaller than spectrum (a), and this indicates that the discharge and charge behaviour have improved after the first cycle. The principal reason for this improvement may lie in the fact that the interfacial properties are improved after discharge/charge of the cell. The observation that the discharge capacity increases from the second cycle should be partly related to the above explanation. The impedance experiment was also performed on the cell after 46 charge/discharge cycles. The results (Fig. 6) show clearly that the composition of the spectrum does not change substantially, even though the semi-circle at low frequency is enlarged. Analysis of the impedance experiments demonstrates that this type of spinel structure material has good Li$^+$ intercalation and de-intercalation characteristics for rechargeable lithium batteries.

4. Conclusions

The spinel structure of an LiMn$_2$O$_4$ positive electrode for use in lithium rechargeable batteries has been prepared and investigated by cyclic voltammetry (CV) and a.c. impedance. The spinel structure of the LiMn$_2$O$_4$ can be obtained easily if the reaction temperature is controlled at 700 or 800 °C for over 50 h under the conditions of a slow rate of temperature increase.

The CV results show that Li$^+$ ions can be intercalated and de-intercalated reversibly. The CV peaks display a split phenomenon. This is due to interaction between the intercalated Li$^+$ ions. Analyses of the impedance of an Li/electrolyte/LiMn$_2$O$_4$ cell shows that the semi-circle is gradually changed to a 'spur' as discharge of the cell proceeds to greater depths. This implies that the diffusion of Li$^+$ ions from the electrolyte into the spinel electrode becomes more difficult and that the surface morphology of the cathode is changing. On the other hand, the impedance spectrum can be virtually recovered after the cell is charged to the original OCV. The capacity of an Li/EC–DEC–LiPF$_6$/LiMn$_2$O$_4$ cell declines from the maximum value of 129 to 113 mAh g^{-1} after 46 charge/discharge cycles.

References

[1] M.M. Thackeray, W.I.F. David, P.G. Bruce and J.B. Goodenough, *Mater. Res. Bull.*, *18* (1983) 461.
[2] M.M. Thackeray, P.J. Johnson, L.A. de Piciotto, P.G. Bruce and J.B. Goodenough, *Mater. Res. Bull.*, *19* (1984) 179.
[3] J.M Tarascon, W.R. McKinnon, F. Coowar, T.N. Bowmer, G. Amatucci and D. Guyomard, *J. Electrochem. Soc.*, *141* (1994) 1421.
[4] J.M. Tarascon and D. Guyomard, *J. Electrochem. Soc.*, *138* (1991) 2864.
[5] D. Guyomard and J.M. Tarascon, *J. Electrochem. Soc.*, *139* (1992) 937.
[6] F.B. Hildebrand, *Advanced Calculus for Application*, Prentice Hall, Englewood Cliffs, 1962, p. 513.